Ab Initio Calculations to Model Anomalous Fluorine Behavior

Milan Diebel*
Department of Physics, University of Washington, Seattle, Washington 98195-1560, USA
Scott T. Dunham
Department of Electrical Engineering, University of Washington, Seattle, Washington 98195-2500, USA
(Received 7 July 2003; published 6 December 2004)

Implanted fluorine is observed to behave unusually in silicon, manifesting apparent uphill diffusion and reducing diffusion and enhancing activation of boron. In order to investigate fluorine behavior, we calculate the energy of fluorine defect structures in the framework of density functional theory. In addition to identifying the ground-state configuration and diffusion migration barrier of a single fluorine atom in silicon, a set of energetically favorable fluorine defect structures were found (F_nV_m). The decoration of vacancies and dangling silicon bonds by fluorine suggests that fluorine accumulates in vacancy-rich regions, which explains the fluorine redistribution behavior reported experimentally.

DOI: 10.1103/PhysRevLett.93.245901 PACS numbers: 66.30.Jt, 61.72.Tt

As silicon devices enter the nanoscale, ultrashallow and highly electrically active junctions become necessary. The current method of choice to introduce dopants into silicon is ion implantation. During the implant process, the crystal structure of the host material (silicon) gets severely damaged. Subsequent high temperature anneals are required to heal the damage as well as activate the introduced dopants. During such anneals, transient enhanced diffusion (TED) of dopants is observed. Reduction in TED and enhanced dopant activation are of crucial importance for the formation of ultrashallow junctions in future silicon process technology. Experimentally, fluorine (F) has been shown to have beneficial effects, reducing TED for boron (B) and phosphorus (P) [1–5] and enhancing boron activation [1–4]. However, to utilize these benefits effectively, a fundamental understanding of the complex F behavior is necessary, particularly since F shows anomalous diffusion [6]. In this Letter, we present *ab initio* calculations conducted within the framework of density functional theory (DFT), which find energetically favorable fluorine defect structures. These structures suggest a distinct redistribution behavior of F and also explain the beneficial effects of F on B and P TED reduction and enhanced dopant activation.

Jeng *et al.* [6] experimentally investigated the diffusion behavior of F. In their experiment, a subamorphizing dose of 10^{13} cm^{-2} F^+ was implanted at 30 keV and annealed for 30 min at various temperatures. The anomalous fluorine redistribution behavior consists of two key features. First, at temperatures below 550 °C, no noticeable F diffusion takes place, while at higher temperatures, rapid F diffusion is reported. This behavior suggests the formation of strongly bound F complexes, since *ab initio* calculations give a migration barrier of only 0.7–1.3 eV [7,8], which indicates that single F atoms should be highly mobile well below 550 °C. The second part of the anomalous behavior is the shapes of the annealed profiles. Instead of broadening, the annealed profiles sharpen and shift toward the surface.

In order to investigate fluorine behavior in silicon, the energies for various configurations were calculated using the DFT code VASP [9,10] with the Perdew-Wang 1991 generalized gradient approximation functional [11] and ultrasoft Vanderbilt-type pseudopotentials [12,13]. All calculations were performed in a nominally 64 atom supercell with periodic boundary conditions and 2^3 Monkhorst-Pack **k**-point sampling. A large energy cutoff of 320 eV was required due to the electronic properties of F. The structures were fully relaxed to a maximal force of less than 0.005 eV/Å per atom. The calculations were performed using the experimental Si lattice constant of 5.43 Å.

Figure 1 shows the formation energy of various single F configurations as a function of the Fermi level E_F. The analysis of the density of states (DOS) shows that none of the listed F complexes have states in the lower half of the Si band gap. Therefore we conclude that a single F atom prefers to reside in a bond-centered (F_{bc}^+) interstitial site for $E_F \leq E_V + 0.36$ eV, where E_V denotes the top of the valence band. For higher Fermi levels the tetrahedral (F_{tet}^-) interstitial configuration is the ground state. The same reference structures were found by Taguchi and Hirayama [8].

In our analysis, we used the DOS resulting from uncharged supercell calculations to estimate the dominant charge states and associated formation energies for each configuration as a function of the Fermi level. We verified our method of using uncharged supercell results to predict formation energies of charged supercells by comparing with charged supercell calculations for all structures reported in Fig. 1 as well as F_3V (F_6V_2 is neutral for all values of E_F in the band gap). In the case of F_{bc}^+, the predicted value differs by only 0.003 eV. The error for F_{tet}^- is 0.07 eV, which is the largest difference found. The values reported in Fig. 1 are based on the charged super-

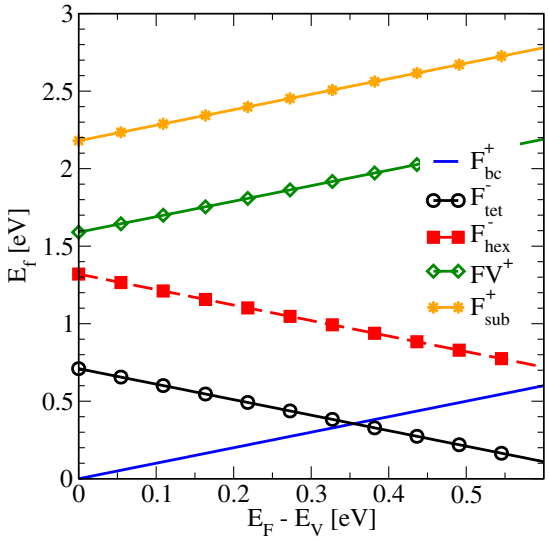

FIG. 1 (color online). Fermi level dependence of formation energies for various single F complexes. All formation energies are in reference to F_{bc}^{-} with the Fermi level at the valence band edge and perfect Si. The formation energy of FV [see Fig. 2 (left panel)] is preferred by 0.59 eV over the symmetric substitutional configuration.

cell calculations for accuracy. In a 64 atom supercell with 2^3 Monkhorst-Pack $\mathbf{k}$-point sampling, the valence band maximum is taken at $\pi/(4a)(1,1,1)$ in the Brillouin zone, which has an energy of 0.2845 eV lower than the valence band maximum at the Γ point. The reported energies for charged F configurations have been corrected accordingly. Previous DFT calculations show interstitial F to be highly mobile ($E_m^{F_{bc}} \leq 1.3$ eV [8], $E_m^{F_{tet}} = 0.7$ eV [7]). We also determined the migration path between different F configurations using the nudged elastic band method [14]. In p-type material, we found the lowest migration path to be $F_{bc}^{+} \rightarrow F_{tet}^{+} \rightarrow F_{bc}^{+}$, where F_{tet}^{+} is an intermediate metastable state of the two-step transition. The associated transition state F_{trans} is also positively charged. In contrast, for n-type material F_{tet}^{-} is the lowest single F energy configuration with a simple one-step migration path. The transition state is almost identical to F_{hex}^{-}. The migration energy between bond-centered sites is $E_m^{F_{bc}^{+}} = 1.38$ eV, whereas the migration barrier for F_{tet}^{-} is 0.60 eV. These results agree well with previous work [7,8]. For midgap Fermi levels, F diffusion will be dominated by F_{tet}^{-} due to lower formation and migration energy.

In addition to fluorine structures, interstitial (I), and vacancy (V) ground-state energies were calculated as references. The calculated formation energies of neutral I ($\langle 110 \rangle$ split) and V are 3.78 and 3.38 eV, respectively, consistent with previous work [15].

We found F_nV_m structures to have a rather high binding energy, suggesting decoration of vacancies by fluorine. The passivation of Si dangling bonds by fluorine is known from surface studies [16]. For substitutional F, the F is shifted away from the lattice site toward one of the neighboring Si atoms [see Fig. 2 (left panel)], which indicates that this structure is more accurately considered a F interstitial decorating a vacancy (FV). In Table I, the formation and binding energies for different F_nV_m configurations are listed. Here the reference point for the total binding energy is negatively charged tetrahedral fluorine (F_{tet}^{-}) and single neutral vacancies. The Fermi level was assumed to be the intrinsic Fermi level at 650 °C ($E_F = E_V + 0.45$ eV [17]).

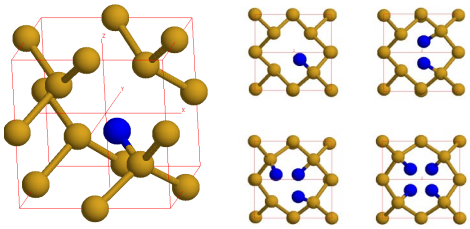

FIG. 2 (color online). Left: 3D view of a neutral single FV complex. The fluorine atom has moved toward one silicon atom out of the substitutional site. The Si-F bond length is 1.68 Å (71% of the Si-Si bond length). The silicon atoms are drawn in amber (light grey), while the fluorine atom is presented in blue (dark grey). Right: A view down the $\langle 100 \rangle$ direction (see left panel) of the four neutral F_nV structures. An increasing distortion of the surrounding silicon lattice is observed when adding more fluorine atoms. This is due to the repulsion of the F atoms, which becomes particularly apparent by comparing FV with the other clusters. Simultaneously, the Si-F bond length is reduced from 1.68 in FV to 1.57 Å in F_4V.

TABLE I. Binding energies of F_nV_m configurations for $E_F = E_V + 0.45$ eV (intrinsic Fermi level at 650 °C [17]). For midgap Fermi level, the clusters are predominantly charge neutral. The decreasing binding energy of the F_nV structures is attributed to the increasing crowding of the F atoms. This phenomenon is illustrated in Fig. 2 (right panel). The total binding energies (third column) are calculated with respect to lowest energy interstitial fluorine configuration for the mentioned Fermi level (F_{tet}^{-}) and single vacancies (V). The binding energies in the second column are the energy change upon adding the final F to the structure. The fourth column lists the total formation energy, which includes the formation energy of the necessary vacancies.

Structure	E_b last F [eV]	E_b^{tot} [eV]	E_f [eV]
V			+3.38
FV	−1.95	−1.95	+1.43
F_2V	−1.80	−3.75	−0.37
F_3V	−1.51	−5.26	−1.88
F_4V	−0.10	−5.36	−1.98
V_2		−1.45	+5.31
FV_2	−2.31	−3.77	+3.00
F_2V_2	−2.43	−6.20	+0.57
F_3V_2	−1.78	−7.98	−1.21
F_4V_2	−1.76	−9.74	−2.98
F_5V_2	−1.59	−11.33	−4.57
F_6V_2	−1.13	−12.46	−5.69

The formation energy of FV was used to estimate the error due to the finite energy cutoff, cell size, and **k**-point sampling. Increasing the cutoff to 450 eV resulted in a change in formation energy on the order of 0.02 eV. Changing the cell size to a 216 atom supercell while leaving the cutoff and **k**-point sampling unchanged led to a change in energy of 0.13 eV. We also increased the **k**-point sampling from 2^3 to 4^3 using the 64 atom supercell with a 500 eV cutoff. The resulting change in formation energy was 0.025 eV.

For two or more F atoms, F_nV_m structures are favored over the interstitial configuration. For F_nV_m structures, the binding energy gained by adding additional fluorine atoms decreases. This behavior is due to the increasing space requirement of the decorating fluorine atoms. This becomes particularly apparent by comparing F_2V with F_3V in Fig. 2 (right panel). Three fluorine atoms in F_3V are pushed away from each other and a distortion of the surrounding silicon lattice is noticeable. The rather large drop in marginal binding energy between F_3V and F_4V from 1.51 to 0.10 eV can be explained with the same argument, since F_4V shows an increasing distortion of the lattice and reduction of the Si-F bond length [see Fig. 2 (right panel)].

We also investigated F_nV_2 structures, which show a similar reduction in binding energy with n, but no sharp drop off, since more space is available to accommodate F atoms at all six dangling bonds. In Fig. 3, the estimated equilibrium concentrations at 650 °C of F structures versus total F concentration are shown (changes in formation entropy are neglected). In the presence of nonequilibrium point-defect concentrations, the local equilibrium F_nV_m concentrations need to be multiplied by $(C_V/C_V^*)^m$. C_V denotes the actual vacancy concentration, whereas C_V^* is the vacancy concentration in equilibrium. Thus, in the presence of excess vacancies during the initial stages of implant annealing, almost all fluorine will reside in F_nV_m structures. The evolution of F_nV_m clusters is particularly important during implant anneals due to the high point-defect concentrations.

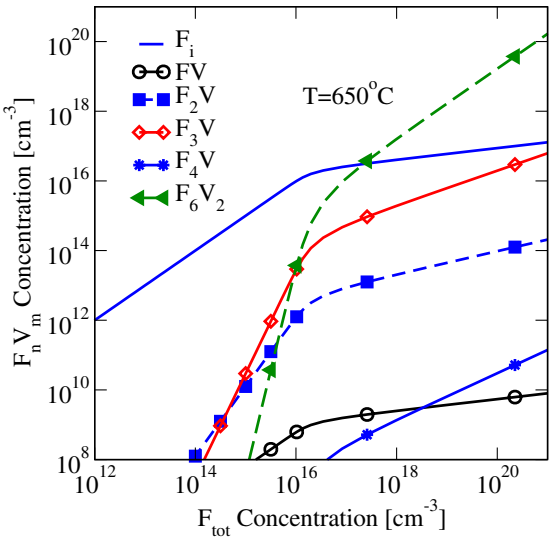

FIG. 3 (color online). Equilibrium concentration of various F_nV_m structures versus total F concentration at 650 °C. The Fermi level is assumed to be at midgap (0.45 eV above the valence band edge [17]). For low $C_{F_{tot}}$, the dominant species is F_i due to the entropy of mixing. At high $C_{F_{tot}}$, the major F contribution comes from F_6V_2 clusters. The vacancy formation energy is included in these calculations.

The saturated F_6V_2 structure shows another interesting property: it is almost stable even in the presence of an interstitial. Table II lists the energy change associated with I reactions with F_nV_m structures. Migration and/or reaction barriers, which might further stabilize F_nV_m structures, are not included. Because of the strong binding of the fluorine atoms with the silicon atoms surrounding vacancies, we believe these defects to be effectively immobile.

All F_nV_m calculations were performed with uncharged supercells. The dependences of the formation energies on the Fermi level were extracted from the DOS [18]. For midgap Fermi levels, the dominant clusters (F_nV and F_6V_2) are all uncharged. Table I lists the formation energies under those conditions. The analysis for incompletely F decorated F_nV_2 clusters is very complicated since they have many gap states, which are introduced by the divacancy V_2.

We also investigated pairing of F_i with I and F_i. DFT predicts interstitial F_2 to be unbound, as the fluorine prefers to remain in an interstitial site rather than forming a F_2 bound state. F_i binds to I with an energy of 0.46 eV. This number was deduced by comparing FI to F_i and I separated within the same supercell.

A recent study by Pi *et al.* [19] using positron annihilation, secondary-ion mass spectroscopy, and cross-

TABLE II. Stability of the F_nV_m cluster in the presence of I. ΔE is defined as $E_f^{F_nV_m} + E_f^I - E_f^{rhs}$. $E_f^{F_nV_m}$ and E_f^I denote the formation energies of F_nV_m and I, respectively, whereas E_f^{rhs} is the total formation energy for the components on right-hand side of the respective reaction. Our calculations find that the fully saturated F_6V_2 structure is effectively stable even at high I concentrations. This calculation does not include possible migration or reaction barriers, which further stabilize F_nV_m structures.

$F_nV + I \Leftrightarrow nF_i$	ΔE [eV]
$n = 1$	+5.21
$n = 2$	+3.41
$n = 3$	+1.90
$n = 4$	+1.80
$F_nV_2 + I \Leftrightarrow F_4V + (n-4)F_i$	ΔE [eV]
$n = 4$	+2.78
$n = 5$	+1.19
$n = 6$	+0.07

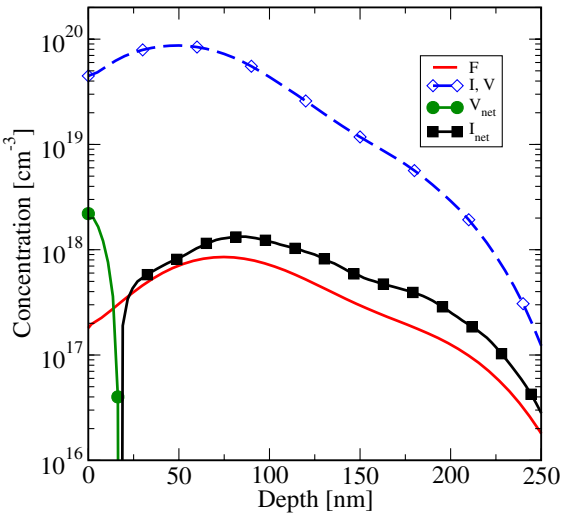

FIG. 4 (color online). As-implanted fluorine and defect profiles of a 10^{13} cm^{-2} 30 keV F implant using Monte Carlo implant simulator UT-MARLOWE [20] showing a vacancy-rich region ($V_{\text{net}} = V - I$) near the surface.

section transmission electron microscopy concludes (in agreement with our calculations) that F forms F_nV_m complexes by decorating the dangling bonds of vacancy clusters. They also observe that F retards I-V recombination, which is a direct conclusion of our calculations. Pi *et al.* analyzed the initial stages of F redistribution and attributed the observed behavior to a F vacancy diffusion mechanism with an activation energy of 2.19 eV. Based on our *ab initio* calculations, we predict a similar activation energy for fluorine migration. However, we attribute the redistribution of F to release and diffusion of F interstitials rather than diffusion of FV complexes. The binding energy for the last F atom added to a F_6V_2 cluster is -1.13 eV, which can be combined with the calculated F_i migration barrier of 0.60 eV to give a predicted activation energy for F migration of 1.73 eV.

In conclusion, *ab initio* calculations predict strongly bound F_nV_m clusters. No other comparably stable structures were identified; the binding energy found for FI clusters is significantly smaller. This DFT data can be used to identify the diffusion mechanism and explain the anomalous fluorine behavior reported by Jeng *et al.* [6]. Fast diffusing F_i decorate V_n forming immobile F_nV_m clusters. At higher temperatures, these clusters are annihilated by I. Figure 4 shows the as-implanted F and point-defect profiles. F decoration of V leads to F dissolving from deeper regions (I excess) and accumulation near the surface (V excess).

Because of the strong affinity of F for V, in preamorphized samples we expect incorporation of F_nV_m clusters during regrowth. The consequences for boron diffusion in such an environment would be TED reduction and activation for amorphizing conditions due to excess V. However, in the case of nonamorphizing implants, we expect an increased I concentration due to the formation of F_nV_m clusters, which leads to an enhancement of TED. These predictions for amorphizing conditions are supported by experimental data [1,2,5].

This research was funded by the Semiconductor Research Corporation (SRC). The authors like to thank Intel Corporation for donation of a computing cluster used in this work.

*Electronic address: diebel@u.washington.edu

[1] T. H. Huang, H. Kinoshita, and D. L. Kwong, Appl. Phys. Lett. **65**, 1829 (1994).
[2] D. F. Downey, J.W. Chow, E. Ishida, and K. S. Jones, Appl. Phys. Lett. **73**, 1263 (1998).
[3] H.W. Kennel, S. M. Cea, A. D. Lilak, P. H. Keys, M. D. Giles, J. Hwang, J. S. Sandford, and S. Corcoran, in *Proceedings of the IEDM 2002 Digest, International Electron Devices Meeting, 2002* (IEEE, Piscataway, NY, 2002), p. 875.
[4] J. Park and H. Hwang, Mater. Res. Soc. Symp. Proc. **568**, 71 (1999).
[5] L. S. Robertson, P. N. Warnes, K. S. Jones, S. K. Earles, M. E. Law, D. F. Downey, S. Falk, and J. Liu, Mater. Res. Soc. Symp. Proc. **610**, B4.2.1 (2000).
[6] S.-P. Jeng, T.-P. Ma, R. Canteri, M. Anderle, and G.W. Rubloff, Appl. Phys. Lett. **61**, 1310 (1992).
[7] C. G. Van de Walle, F. R. McFeely, and S. T. Pantelides, Phys. Rev. Lett. **61**, 1867 (1988).
[8] A. Taguchi and Y. Hirayama, Solid State Commun. **116**, 595 (2000).
[9] G. Kresse and J. Hafner, Phys. Rev. B **47**, 558 (1993).
[10] G. Kresse and J. Furthmüller, Phys. Rev. B **54**, 11 169 (1996).
[11] J. P. Perdew, J. A. Chevary, S. H. Vosko, K. A. Jackson, M. R. Pederson, D. J. Singh, and C. Fiolhais, Phys. Rev. B **46**, 6671 (1992).
[12] D. Vanderbilt, Phys. Rev. B **41**, 7892 (1990).
[13] G. Kresse and J. Hafner, J. Phys. Condens. Matter **6**, 8245 (1994).
[14] H. Jónsson, G. Mills, and K.W. Jacobsen, *Classical and Quantum Dynamics in Condensed Phase Simulations* (World Scientific, Singapore, 1998), p. 385.
[15] B. P. Uberuaga, Ph.D. thesis, University of Washington, 2000.
[16] B. R. Weinberger, H.W. Deckman, E. Yablonovitch, T. Gmitter, W. Kobasz, and S. Garoff, J. Vac. Sci. Technol. A **3**, 887 (1985).
[17] A. L. Smith, S. T. Dunham, and L. C. Kimerling, Physica (Amsterdam) **273B**, 358 (1999).
[18] M. Diebel, Ph.D. thesis, University of Washington, 2004.
[19] X. D. Pi, C. P. Burrows, and P. G. Coleman, Phys. Rev. Lett. **90**, 155901 (2003).
[20] S. Tian *et al.*, computer code UT-MARLOWE 5.1, University of Texas at Austin, 2001.